Pis'ma v ZhETF, vol. 102, iss. 8, pp. 558 – 564

Coherent control of optical bistability and multistability in a triple semiconductor quantum well nanostructure

A. Raheli[1)]+, *H. Afshari*[*], *H. R. Hamedi*[×1)]

[+]*Department of Physics, Bonab Branch, Islamic Azad University, Bonab, Iran*

[*]*Research Institute for Applied Physics, University of Tabriz, Tabriz, Iran*

[×]*Institute of Theoretical Physics and Astronomy, Vilnius University, A. Goštauto 12, Vilnius LT-01108, Lithuania*

Submitted 10 August 2015
Resubmitted 26 August 2015

This paper deals with optical bistability (OB) and optical multistability (OM) behaviors for a triple semiconductor quantum well (SQW) structure driven coherently with two control fields, confined in an unidirectional ring cavity. The effect of different system parameters on OB and OM is explored. It is found that the threshold of onset of the OB can be controlled by manipulating the Rabi-frequency of control fields. In this case, OB can be converted to OM. Then we investigate the effect of probe and control field detunings on OB behaviors. We found that the frequency detuning of probe field affects only the upper-lower branches of the OB curves but has no specific impact on OB threshold. By manipulating the first control field detuning, neither the OB threshold intensity nor upper-lower branches change. Finally, it is found that increasing the second control field detuning can reduce merely the OB threshold intensity, while no change happens in upper-lower OB branches. The results may be applicable in real experiments for realizing an all-optical switching or coding element in a solid-state platform.

DOI: 10.7868/S0370274X15200035

1. Introduction. Quantum coherence and interference can be utilized to explore various possibilities, ranging from linear and nonlinear optics [1–24]. Optical bistability (OB), which appears in nonlinear optical systems surrounded by loop of feedback, is a feature in which two stable output intensities are often accessible for a single input intensity (one large and one small). During the past several decades, there has been a lot of attention paid to the optical bistability due to its implementation in all-optical transistors, switches, logical gates, and memories [25–35].

There is also a significant interest in quantum coherence based-phenomena in semiconductor quantum dots (SQD) and semiconductor quantum wells (SQW) [36–59].

SQDs exhibit properties similar to atomic vapours but with the advantage of high nonlinear optical coefficients, large electric-dipole moments of intersubband transitions due to the small effective electron mass as well as ease of integration. Many ideas have been proposed and analyzed in SQDs. For instance, Mantsevich et al. [53] investigated the peculiarities of nonequilibrium charge configurations in the system of two strongly coupled quantum dots weakly connected to the reservoirs in the presence of Coulomb correlations and revealed that total electron occupation demonstrates in some cases significant decreasing with increasing of applied bias. In another work with the same group, external field induced switching of tunneling current in the coupled quantum dots was investigated [54]. The out-of-equilibrium transport properties of a double quantum dot system in the Kondo regime is theoretically investigated with Orellana and colleagues [56]. The behavior of bistability in quantum-dot structures is also studies via a drift-diffusion model in combination with electron capture and emission processes [57]. Other studies deal with investigation on bistable tunneling current through a molecular quantum dot [58], bistable spin currents from quantum dots embedded in a microcavity [59], and so on.

Intersubband transition-based devices in the SQWs have also many intrinsic advantages that the atomic systems do not have, such as the large electric dipole moments due to the small effective electron mass, the great flexibilities in devices design by choosing the materials and structure dimensions, the high nonlinear optical coefficients. Furthermore, the transition energies, the dipoles as well as the symmetries can also be engineered as desired [60]. On the basis of their impor-

[1)]e-mail: Raheliali.b@gmail.com; raheliali@yahoo.com; hamid.r.hamedi@gmail.com; hamid.hamedi@tfai.vu.lt

tant properties, several works have been performed on quantum interference and coherence based phenomena in SQWs. For example, Peng and co-workers have investigated the optical precursors with tunneling-induced transparency in asymmetric quantum wells [50]. Recently, the absorption-dispersion properties of a weak probe laser field for a triple SQW structure driven coherently by two control laser fields have been analyzed by Yang et al. [52]. They have shown that such SQW structure can produce anomalous and normal dispersion regions with negligible absorption by adjusting the intensities of the control fields. Now, in this letter, we intend to study the optical bistability and optical multistability (OM) behaviors for such triple SQW structure inside a unidirectional ring cavity. We show that by suitably varying the intensity and frequency detuning of control laser fields, the controllability of OB and OM is possible for such SQW model. Note that we will not consider the influence of Fano-interference in present work, as it could be the subject of another work. The paper is organized as follows: Secs. 1 and 2 provide the introduction, and the description of proposed model and related equations, respectively. In Sec. 3, we give the numerical results, and finally, Sec. 4 represents the conclusion.

2. Model and Equations. The schematic band diagram of the triple semiconductor quantum well including a deep well and two shallow wells coupled by tunneling to a common continuum of energies through a thin barrier, and the corresponding energy levels are shown in Figs. 1a and b, respectively. Such structure can be obtained, as discussed in Ref. [37], by coupling two shallow $Al_{0.2}Ga_{0.8}As$ wells with thickness of 6.8-nm separated by a 2.0-nm-thick $Al_{0.4}Ga_{0.6}As$ barrier and a deep 7.1-nm-thick GaAs well to a common continuum ($Al_{0.165}Ga_{0.835}As$) through a 0.7-nm-thick $Al_{0.4}Ga_{0.6}As$ Al barrier. The deep well is separated from the second shallow well by an $Al_{0.4}Ga_{0.6}As$ barrier with 2.5 nm thickness. The electronic levels of the ground state and three excited states are denoted by $|1\rangle$, $|2\rangle$, $|3\rangle$, and $|4\rangle$, respectively. A probe field with Rabi frequency Ω_p and angular frequency ω_p mediates the transition $|1\rangle \to |2\rangle$. Two coherent control fields with Rabi frequencies Ω_c, Ω_l and angular frequencies ω_c, ω_l are applied to the transitions $|1\rangle \leftrightarrow |3\rangle$ and $|1\rangle \leftrightarrow |4\rangle$, respectively.

The density-matrix equations of the motion for the SQW structure in dipole and rotating-wave approximations can be written as

$$i\dot{\rho}_{22} = i\gamma_2\rho_{22} - \Omega_p(\rho_{21} - \rho_{12}),$$

$$i\dot{\rho}_{33} = i\gamma_3\rho_{33} + \Omega_c(\rho_{13} - \rho_{31}),$$

$$i\dot{\rho}_{44} = i\gamma_4\rho_{44} - \Omega_l(\rho_{41} - \rho_{14}),$$

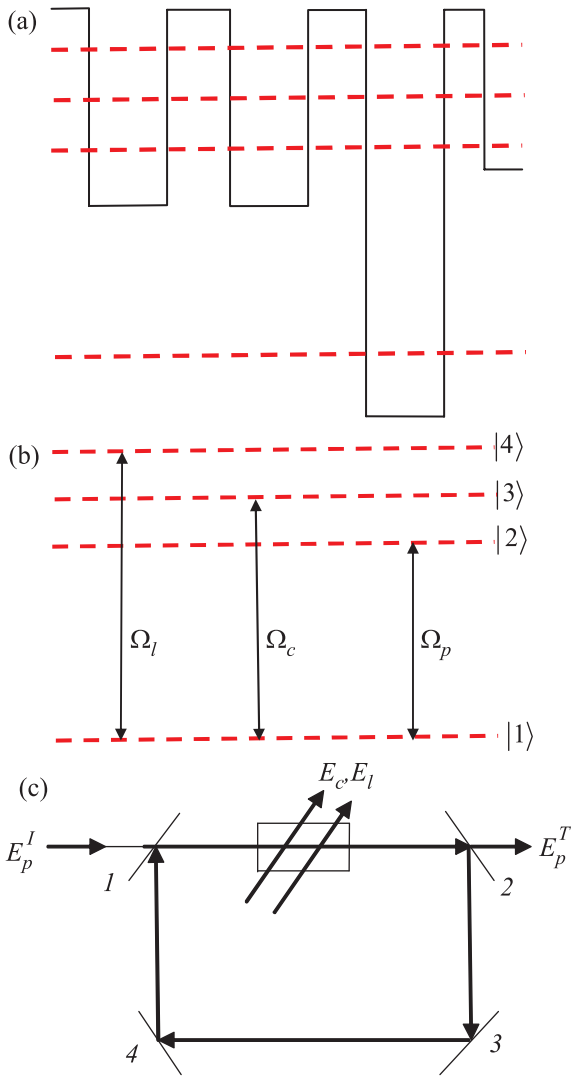

Fig. 1. (Color online) (a) – Schematic band diagram of the SQW structure consisting of a deep well and two shallow wells coupled by tunneling to a common continuum of energies through a thin barrier. (b) – Schematic of related energy levels. (c) – Unidirectional ring cavity with atomic sample of length L. E_P^I and E_P^T are the incident and transmitted fields, respectively. E_1 and E_2 are the strong coupling fields. For mirrors *1* and *2* we have $R + T = 1$. Mirrors *3* and *4* are perfect reflectors. Possible arrangement of experimental apparatus containing an atomic sample of length L. E_p, E_c, E_{RF} represent a weak pulsed probe field, a strong cw control field and a tunable RF-driving field, respectively

$$i\dot{\rho}_{41} = (\Delta_l - i\gamma_{41})\rho_{41} + \Omega_l(\rho_{11} - \rho_{44}) - \Omega_p\rho_{42} - \Omega_c\rho_{43},$$

$$i\dot{\rho}_{24} = (\Delta_l - \Delta_p - i\gamma_{24})\rho_{24} - \Omega_l\rho_{21} - \Omega_p\rho_{14},$$

$$i\dot{\rho}_{43} = (\Delta_l - \Delta_c - i\gamma_{43})\rho_{43} + \Omega_l\rho_{13} - \Omega_c\rho_{41},$$

$$i\dot{\rho}_{23} = (\Delta_c - \Delta_p - i\gamma_{23})\rho_{23} - \Omega_c\rho_{21} + \Omega_p\rho_{13},$$

$$i\dot{\rho}_{13} = (\Delta_c - i\gamma_{13})\rho_{13} - \Omega_c(\rho_{11} - \rho_{33}) - \Omega_p\rho_{23} + \Omega_l\rho_{43},$$

$$i\dot{\rho}_{21} = (\Delta_p - i\gamma_{21})\rho_{21} + \Omega_p(\rho_{11} - \rho_{22}) - \Omega_c\rho_{23} - \Omega_l\rho_{24},$$

where $\rho_{ij} = \rho^*_{ji}$, $\sum_{i=1}^{4} = \rho_{ii} = 1$. The half-Rabi frequencies are $\Omega_k = \mathcal{P}_{ij}E_k/2\hbar$ (i, j = 1, 2, 3, 4; $i \neq j$; $k = p, c, l$) with E_k and $\mathcal{P}_{ij}$ being the corresponding electric field amplitude and the dipole matrix element induced on the transition $|i\rangle \leftrightarrow |j\rangle$, respectively. Note that $\Delta_p = (\varepsilon_2 - \varepsilon_1)/\hbar - \omega_p$, $\Delta_c = (\varepsilon_3 - \varepsilon_1)/\hbar - \omega_c$, $\Delta_l = (\varepsilon_4 - \varepsilon_1)/\hbar - \omega_l$, are the detuning of the corresponding applied fields (ε_j being the energy of state $|j\rangle$). In addition, the decay rates are included phenomenologically in the above equations. The total decay rates γ_{ij} ($i \neq j$) are: $\gamma_{21} = (\gamma_2 + \gamma_{21}^{dph})/2$, $\gamma_{23} = (\gamma_2 + \gamma_3 + \gamma_{32}^{dph})/2$, $\gamma_{13} = (\gamma_3 + \gamma_{31}^{dph})/2$, $\gamma_{41} = (\gamma_4 + \gamma_{41}^{dph})/2$, $\gamma_{24} = (\gamma_2 + \gamma_4 + \gamma_{42}^{dph})/2$, and $\gamma_{43} = (\gamma_4 + \gamma_3 + \gamma_{43}^{dph})/2$, where γ_j ($j = 2, 3, 4$) are the population scattering rates which are primarily due to the longitudinal optical phonon emission events at low temperature [61] and the pure dipole dephasing rates γ_{ij}^{dph} are considered to be a combination of quasi-elastic interface roughness scattering or acoustic phonon scattering [49, 62]. One can calculate the population decay rates by solving the effective mass Schrödinger equation. For the temperatures up to 10 K, the dephasing decay rates γ_{ij}^{dph} can be estimated based on Refs. [37, 48]. For our model, they are $\gamma_2 = 1.32$ meV, $\gamma_3 = 1.72$ meV, $\gamma_4 = 2.24$ meV, and $\gamma_{21}^{dph} = \gamma_{31}^{dph} = \gamma_{41}^{dph} = \gamma_{32}^{dph} = \gamma_{42}^{dph} = \gamma_{43}^{dph} = 1.65$ meV. A general treatment of the decay rates would involve incorporation of the decay mechanisms into the Hamiltonian of the system. However, we have adopted the phenomenological approach of treating the decay mechanisms just as done in Ref. [15, 16, 62]. A more fully two-dimensional treatment taking into account these processes has been investigated quite thoroughly by some authors (for example [63, 64]).

According to the standard model of Bonifacio and Lugiato [65], a medium of length L composed of the proposed SQW sample immersed in an unidirectional ring cavity is considered. We assume that both the mirrors *3* and *4* are perfect reflectors, and the reflection and transmission coefficients of mirrors *1* and *2* are R and T (with $R + T = 1$), respectively.

Under slowly varying envelop approximation, the dynamics response of the probe field is governed by Maxwell's equation

$$\frac{\partial E_p}{\partial t} + \nu_F\frac{\partial E_p}{\partial z} = \frac{i\omega_p}{2\varepsilon_r}P(\omega_p), \tag{2}$$

where $P(\omega_p)$ shows the induced polarization. For a perfectly tuned cavity, the boundary conditions in the steady-state limit between the incident field E_1^I and transmitted field E_1^T are [26]:

$$E_1(L) = \frac{E_1^T}{\sqrt{T}}, \tag{3a}$$

$$E_1(0) = \sqrt{T}E_1^I + RE_1(L), \tag{3b}$$

where L describes the length of the sample. The second term on the right-hand side of Eq. (3b) is the feedback mechanism due to the reflection from mirrors, essential for the bistability. When $R = 0$ in Eq. (3b), bistable behavior is expected. In line with the mean-field limit, and using the boundary condition, the steady state behavior of elliptically polarized transmitted field reads

$$Y = 2x - iC\rho_{21}, \tag{4}$$

where $y = \mathcal{P}_{21}E_1^I/\hbar\sqrt{T}$ and $x = \mathcal{P}_{21}E_1^T/\hbar\sqrt{T}$ are the normalized input and output field, respectively. The parameter $C = N\omega_p L\mathcal{P}_{21}^2/2\hbar\varepsilon_0 cT$ is the electronic cooperatively parameter. Transmitted field depends on the incident probe field and the coherence terms ρ_{21} via Eq. (4). The coherence term ρ_{21} given in Eq. (4) is obtained from probe susceptibility $\chi_{21} = \frac{2N|\mathcal{P}_{21}|^2}{\varepsilon_0\hbar\Omega_p}\rho_{21}$, where here, N is the electron density in the conduction band.

Assuming that system is populated predominantly in the ground state $|1\rangle$, and since the driving fields are assumed to be strong compared to the probe field, the analytical solution for the coherence term ρ_{21} can be expressed as

$$\rho_{21}^{(1)} = i\Omega_p\frac{x_1x_2}{x_2\Omega_c^2 + x_1\Omega_l^2 + x_1x_2x_3}, \tag{5}$$

where

$$x_1 = \Delta_c - \Delta_p - i\gamma_{23},\ x_2 = \Delta_l - \Delta_p - i\gamma_{24},\ x_3 = \Delta_p - i\gamma_{21}.$$

The imaginary part of ρ_{21} related to the probe susceptibility shows the absorption of probe field for the SQW medium.

3. Numerical results and discussions. In the following, the behavior of optical bistability for the system under consideration will be analyzed thoroughly.

Eqs. (4) and (5) show that the OB is dependent on the controllable parameters of the SQW system, i.e., the intensity and detuning of the laser fields. As a result, one can control the OB behaviors through proper adjusting the system parameters.

We display the numerical simulations in Figs. 2–5.

First, we explore how the intensity of the Rabi-frequency Ω_c affects the bistable behavior of SQW sample. The input-output field curves for different values

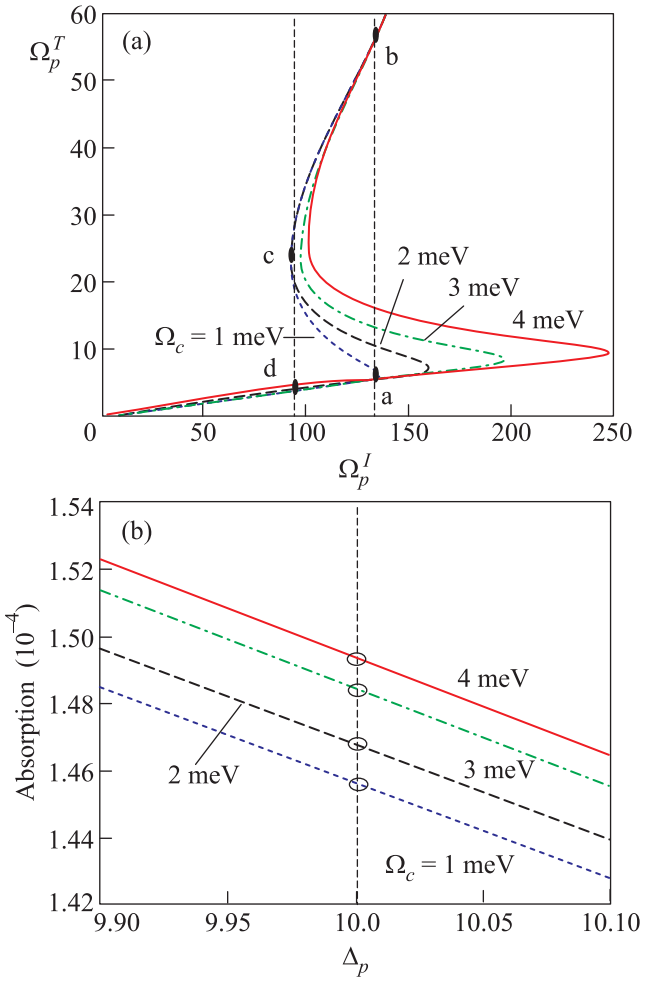

Fig. 2. (Color online) Plots of the input-output field curves (a) and probe absorption for different values of Ω_c (b). The selected parameters are, $\gamma_2 = 1.32$ meV, $\gamma_3 = 1.72$ meV, $\gamma_4 = 2.24$ meV, and $\gamma_{21}^{dph} = \gamma_{31}^{dph} = \gamma_{41}^{dph} = \gamma_{32}^{dph} = \gamma_{42}^{dph} = \gamma_{43}^{dph} = 1.65$ meV, $\Omega_p = 0.001$ meV, $\Omega_i = 1$ meV, $\Delta_c = \Delta_l = 1$ meV, $\Delta_p = 10$ meV, $C = 500$

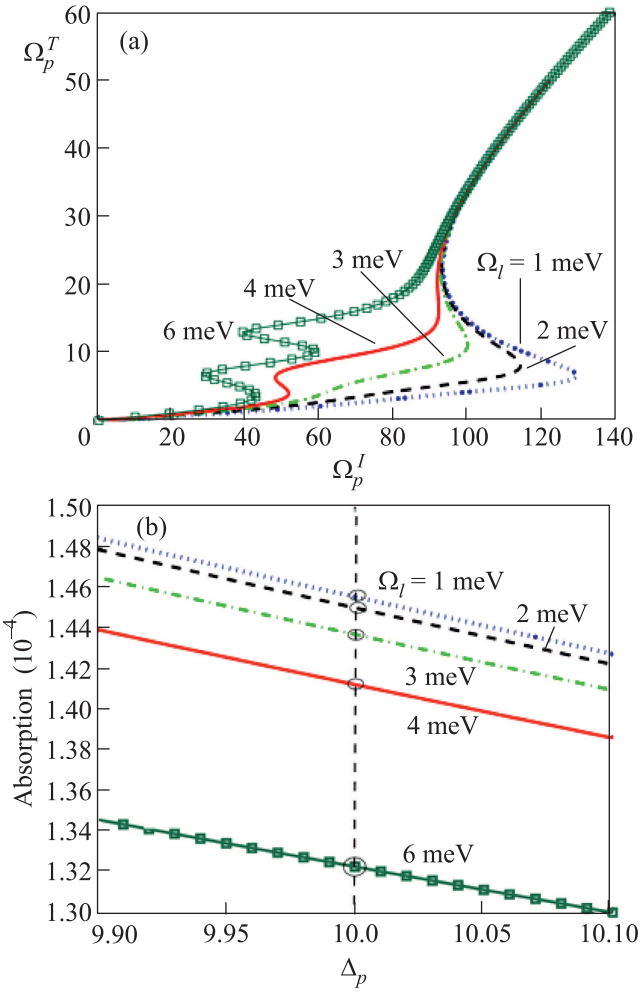

Fig. 3. (Color online) Plots of the input-output field curves (a) and probe absorption for different values of Ω_l (b). Here, $\Omega_c = 1$ meV, and the selected parameters are the same as Fig. 2

of Ω_c are plotted in Fig. 2a. Let us firstly consider the blue dot-line related to the $\Omega_c = 1$ meV. As can be observed, when starting from lower powers, there exists a sudden jump in the output field intensity from the turning point a in the lower branch to the point b located in upper branch. Another jump occurs in the contrariwise regime (starting from higher powers and decreasing it) and from the turning point c to the point d in lower branch. This hysteresis behavior gives rise to the optical bistability.

In addition, it can be seen that by increasing the intensity of Ω_c to $\Omega_c = 2$ meV (black dash-line), $\Omega_c = 3$ meV (green dash-dot-line), and then $\Omega_c = 4$ meV (red solid-line), the threshold of optical bistability can be remarkably increased. The main reason for this behavior could be attributed to the enhancement of absorption for the system at the probe detuning $\Delta_p = 10$ meV. Fig. 2b shows that increasing the intensity of Ω_c increases the probe absorption value at $\Delta_p = 10$ meV which support our comment.

The effect of the Rabi-frequency Ω_l on optical bistability behavior of the sample is shown in Fig. 3a. As can be seen, increasing Ω_l results in different behavior of OB threshold with respect to Fig. 2; the OB threshold is reduced by increasing Ω_l. In addition, when we change Ω_l from 3 to 4 meV, the OB switches to OM. Note that switching between OB and OM is an interesting result due to its potential application in all-optical switching or coding elements. We found that by more increasing of Ω_l (e.g., $\Omega_l = 6$ meV), the OM threshold intensity is reduced more. The main reason for switching between OB and OM is related to Eq. (4). By increasing the in-

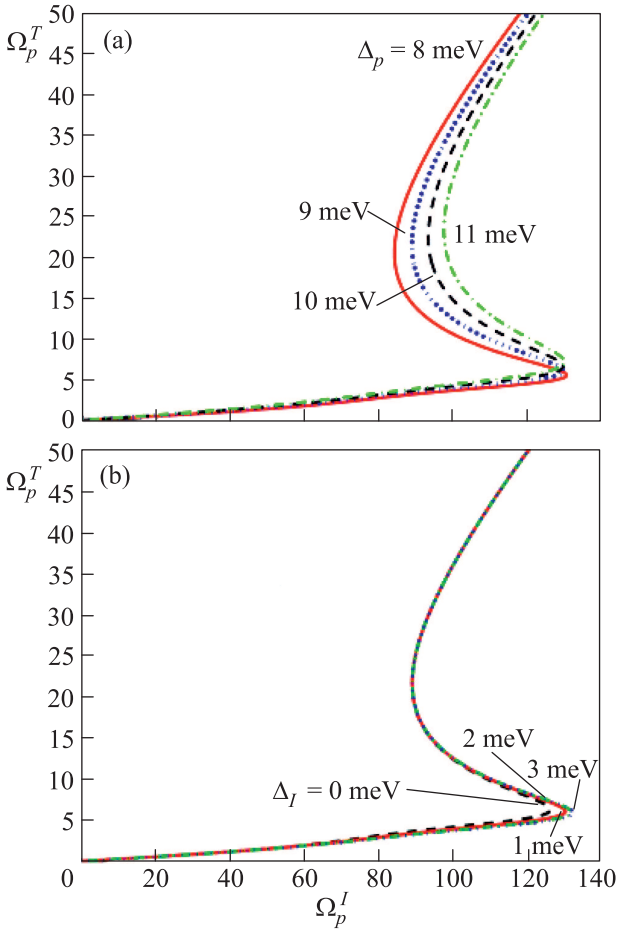

Fig. 4. (Color online) Plots of the input-output field curves for different values of Δ_p (a) and Δ_l (b). The selected parameters are the same as Fig. 2

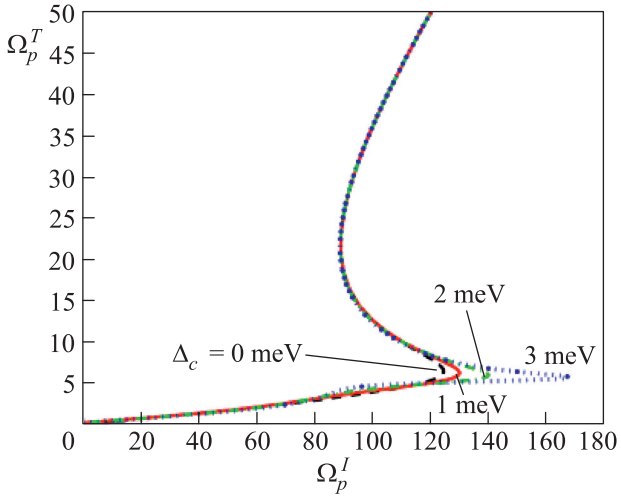

Fig.5. (Color online) Plots of the input-output field curves for different values of Δ_c. The selected parameters are the same as Fig. 2

tensity of Rabi frequency Ω_l the order of the variable x in Eq. (4) goes higher for the proposed four-level QW system, which depends on the relative strengths of different parameters associated with the QW system, that is to say, the observed OM may depend on the complicated form of the variable x. Physically, for the small values of Ω_l, the coherence of the medium is not high enough. Increasing Ω_l can increase the coherence of the system which may lead to enhancement of Kerr nonlinearity for the probe field, therefore, we can realize the transition from the OB to the OM through increasing Ω_l.

In order to get the physical origin of such behavior, we plot the absorption profile versus probe detuning for different values of Ω_l. It is obvious that by increasing Ω_l, the value of probe absorption reduces at $\Delta_p = 10$ meV. Thus, the cavity field more easily reaches saturation which enables reduction of the bistable threshold intensity.

Next, we investigate the influence of probe field detuning Δ_p as well as the control field detuning Δ_l on behavior of optical bistability for the proposed SQW model. Fig. 4 illustrates the input-output curves for different values of Δ_p (a) and Δ_l (b). One can observe in Fig. 4a that different values of probe field detuning only affects the lower and upper branches of OB, and do not change the OB threshold intensity. Also, Fig. 4b displays that by modulating Δ_l, neither the OB threshold intensity nor upper-lower branches change. Moreover, OM is never established in these cases.

It is known that in order to be of practical interest, the threshold value of the input intensity for OB curves must be sufficiently reduced [66]. To this end, we show in Fig. 5 the effect of the first control field detuning i.e., Δ_c, on OB features. Obviously, manipulating Δ_c has no specific effect on lower and upper branches of OB, but reduces the threshold of onset of OB curves. This indicates that when the control fields Ω_c are not resonance with the transition $|1\rangle \leftrightarrow |3\rangle$, the absorption-dispersion and the Kerr nonlinearity of the medium can be modified leading to changes in OB threshold reduction threshold intensity. Thus, we found an advantage of utilizing control field detuning Δ_c in this SQW structure in reducing OB threshold intensity rather than using Δ_p and Δ_l.

4. Conclusions. We have investigated the optical bistability and optical multistability for a triple semiconductor quantum well confined in a ring cavity. We analyzed how OB and OM features can be controlled via different system parameters. It is found that the Rabi-frequency of control fields can result in reduction or enhancement of threshold of onset of OB. Moreover, it was

shown numerically that one can control the upper-lower branches of OB curves as well as OB threshold intensity through proper adjusting the frequency detuning of probe and control fields.

H.R.H. gratefully acknowledges the support of Lithuanian Research Council (# VP1-3.1-ŠMM-01-V-03-001).

1. Y. Wu and X. Yang, Phys. Rev. A **70**, 053818 (2004).
2. Y. Wu, M. G. Payne, E. W. Hagley, and L. Deng, Opt. Lett. **29**, 2294 (2004).
3. Y. Wu and X. Yang, Phys. Rev. A **71**, 053806 (2005).
4. Y. Niu and Sh. qing Gong, Phys. Rev. A **73**, 053811 (2006).
5. W.-X. Yang, T.-T. Zha, and R.-K. Lee, Phys. Lett. A **374**, 355 (2009).
6. Y. Wu and X. Yang, Appl. Phys. Lett. **91**, 094104 (2007).
7. H. R. Hamedi, JETP Lett. **100**, 44 (2014).
8. M. Fleischhauer, A. Imamoglu, and J. P. Marangos, Rev. Mod. Phys. **77**, 633 (2005).
9. Y. Gong, J. Huang, K. Li, N. Copner, J. J. Martinez, L. Wang, T. Duan, W. Zhang, and W. H. Loh, Opt. Express **20**, 24030 (2012).
10. H. Ahmad, K. Thambiratnam, N. A. Awang, Z. A. Ghani, and S. W. Harun, Laser Phys. Lett. **9**, 819 (2012).
11. H.-T. Zhang, H. Wang, and Z.-P. Wang, Phys. Scr. **84**, 065402 (2011).
12. J. Li, R. Yu, M. Liu, Ch. Ding, and X. Yang, Phys. Lett. A **375**, 3978 (2011).
13. J. Xu, Q. Li, W.-ch. Yan, X.-d. Chen, and X.-m. Hu, Phys. Lett. A **372**, 6032 (2008).
14. W.-X. Yang, A.-X. Chen, L.-G. Si, K. Jiang, X. Yang, and R.-K. Lee, Phys. Rev. A **81**, 023814 (2010).
15. W.-X. Yang, J.-M. Hou, and R.-K. Lee, Phys. Rev. A **77**, 033838 (2008).
16. W.-X. Yang, J.-M. Hou, Y.Y. Lin, and R.-K. Lee, Phys. Rev. A **79**, 033825 (2009).
17. Zh. Wang and B. Yu, Las. Phys. Lett. **11**, 035201 (2014).
18. A. W. Rahmatullah and S. Qamar, Las. Phys. Lett. **11**, 045202 (2014).
19. R.-G. Wan and T.-Y. Zhang, Opt. Express **19**, 25823 (2011).
20. W. Fei, G. Cheng, T. Xin-Yu, and S. Wen-Xing, Chin. Phys. B **21**(11), 114206 (2012).
21. Ch. Ding, J. Li, X. Yang, D. Zhang, and H. Xiong, Phys. Rev. A **84**(4), 043840 (2011).
22. R.-G. Wan, T.-Y. Zhang, and J. Kou, Phys. Rev. A **87**, 043816 (2013).
23. Zh. Zhu, W.-X. Yang, A.-X. Chen, Sh. Liu, and R.-K. Lee, Josa B **32**(6), 1070 (2015).
24. A. Raheli, H. R. Hamedi, and M. Sahrai, Las. Phys. Lett. **12**, 095201 (2015).
25. H. Chang, H. Wu, Ch. Xie, and H. Wang, Phys. Rev. Lett. **93**, 213901 (2004).
26. J.-H. Li, X.-Y. Lü, J.-M. Luo, and Q.-J. Huang, Phys. Rev. A **74**, 035801 (2006).
27. J. Li, Physica D **228**, 148 (2007).
28. Zh.-H. Xiao and K. Kim, Opt. Comm. **283**(15), 2178 (2010).
29. Zh. Wang, A.-X. Chen, Y. Bai, W.-X. Yang, and R.-K. Lee, JOSA B **29**, 2891 (2012).
30. Z. Wang and B. Yu, J. Luminescence **132**, 2452 (2012).
31. D.-ch. Cheng, Ch.-p. Liu, and Sh.-q. Gong, Phys. Lett. A **332**, 244 (2004).
32. D.-ch. Cheng, Ch.-p. Liu, and Sh.-q. Gong, Opt. Comm. **263**, 111 (2006).
33. H. R. Hamedi, JETP Lett. **100**, 299 (2014).
34. H. R. Hamedi and S. H. Asadpour, J. Appl. Phys. **117**, 183101 (2015).
35. H. R. Hamedi, A. Khaledi-Nasab, A. Raheli, and M. Sahrai, Opt. Comm. **312**, 117 (2014).
36. D. E. Nikonov, A. Imamoğlu, and M. O. Scully, Phys. Rev. B **59**, 12212 (1999).
37. C.-R. Lee, Y.-C. Li, F. K. Men, C.-H. Pao, Y.-C. Tsai, and J.-F. Wang, Appl. Phys. Lett. **86**, 201112 (2005).
38. A. Joshi, Phys. Rev. B **79**, 115315 (2009).
39. A. Imamoğlu and R. J. Ram, Opt. Lett. **19**, 1744 (1994).
40. M. D. Frogley, J. F. Dynes, M. Beck, J. Faist, and C. C. Phillips, Nat. Mater. **5**, 175 (2006).
41. A. Joshi and M. Xiao, Appl. Phys. B **79**, 65 (2004).
42. J. H. Li, Phys. Rev. B **75**, 155329 (2007); J.-H. Li, Opt. Comm. **274**, 366 (2007).
43. H. Sun, S. Gong, Y. Niu, S. Jin, R. Li, and Z. Xu, Phys. Rev. B **74**, 155314 (2006).
44. T. Shui, Zh. Wang, and B. Yu, Phys. Lett. A **378**, 235 (2014).
45. J. F. Dynes, M. D. Frogley, M. Beck, J. Faist, and C. C. Phillips, Phys. Rev. Lett. **94**, 157403 (2005).
46. H. R. Hamedi, Phys. E **66**, 309 (2015).
47. G. B. Serapiglia, E. Paspalakis, C. Sirtori, K. L. Vodopyanov, and C. C. Phillips, Phys. Rev. Lett. **84**, 1019 (2000).
48. J. Li, X. Hao, J. Liu, and X. Yang, Phys. Lett. A **372**, 716 (2008).
49. E. Paspalakis, M. Tsaousidou, and A. F. Terzis, Phys. Rev. B **73**, 125344 (2006).
50. Y. Peng, Y. Niu, Y. Qi, H. Yao, and S. Gong, Phys. Rev. A **83**, 013812 (2011).
51. A. Chen, Opt. Express **22**(22), 26991 (2014).
52. W.-X. Yanga, W.-H. Ma, L. Yang, G.-R. Zhang, and R.-K. Lee, Opt. Comm. **324**, 221 (2014).
53. V. N. Mantsevich, N. S. Maslova, and P. I. Arseyev, Sol. State Comm. **199**, 33 (2014).

54. V. N. Mantsevich, N. S. Maslova, and P. I. Arseyev, JETP Lett. **100**(4), 265 (2014).
55. V. J. Goldman, D. C. Tsui, and J. E. Cunningham, Phys. Rev. Lett. **58**, 1256 (1987).
56. P. A. Orellana, G. A. Lara, and E. V. Anda, Phys. Rev. B **65**, 155317 (2002).
57. A. Rack, R. Wetzler, A. Wacker, and E. Schöll, Phys. Rev. B **66**, 165429 (2002).
58. A. S. Alexandrov, A. M. Bratkovsky, and R. S. Williams, Phys. Rev. B **67**, 075301 (2003).
59. I. Djuric and Ch. P. Searc, Phys. Rev. B **75**, 155307 (2007).
60. H. C. Liu and F. Capasso, *Intersubband Transitions in Quantum Wells Physics and Device Applications*, Academic, N.Y. (2000).
61. S. M. Goodnick and P. Lugli, in *Hot Carriers in Semiconductor Nanostructures*, Academic, San Diego (1992), ch. 3, p. 219.
62. W. Pötz, Phys. Rev. B **71**, 125331 (2005).
63. F. Biancalana, S. B. Healy, R. Fehse, and E. P. O'Reilly, Phys. Rev. A **73**, 063826 (2006).
64. I. Waldmüller, J. Förstner, S.-C. Lee, A. Knorr, M. Woerner, K. Reimann, R. A. Kaindl, T. Elsaesser, R. Hey, and K. H. Ploog, Phys. Rev. B **69**, 205307 (2004).
65. R. Bonifacio and L. A. Lugiato, Phys. Rev. A **18**, 1129 (1978).
66. He and M. Cada, Appl. Phys. Lett. **61**(18), 2150 (1992).